

Torsion Discovery Potential and Its Discrimination at CERN LHC

F. M. L. de Almeida Jr., A. A. Nepomuceno
*Instituto de Física,
Universidade Federal do Rio de Janeiro,
Rio de Janeiro, RJ, Brazil**

M. A. B. do Vale
*Departamento de Ciências Naturais,
Universidade Federal de São João del Rei,
São João del Rei, 36301-160, MG, Brazil †*

Torsion models constitute a well known class of extended quantum gravity models. In this paper we study some phenomenological consequences of a torsion field interacting with fermions at LHC. A torsion field could appear as a new heavy state characterized by its mass and couplings to fermions. These new states will form a resonance decaying into difermions, as occurs in many extensions of the Standard Model, such as models predicting the existence of additional neutral gauge bosons, usually named Z' . Using the dielectron channel we evaluate the integrated luminosity needed for a 5σ discovery as a function of the torsion mass, for different coupling values. We also calculate the luminosity needed for discriminate, with 95% C.L., the two possible different torsion natures. Finally, we show that the observed signal coming from the torsion field could be distinguished from a signal coming from a new neutral gauge boson, provided there is enough luminosity.

PACS numbers: 13.85.-t, 04.60.-m

I. INTRODUCTION

One great challenge of the Standard Model is the difficulty to incorporate gravity. Several alternative theories of quantum gravity, extending general relativity, introduce an extra field called torsion [1, 2, 3], where the spin of the elementary particles is the source of the torsion. In a phenomenological point of view, torsion can be treated as a fundamental propagating field, either of vectorial or pseudo-vectorial nature, characterized by its mass and the coupling values (η_f) between torsion and fermions. Despite there are strong theoretical restrictions on the possible parameters of the propagating torsion field [4], there is still room for detecting this field on high energy colliders. The introduction of torsion fields leads to singularity-free cosmological models [5, 6] and they can be investigated in the near future high energy particle colliders, such as the LHC at CERN, through their interaction with the fermions. Some torsion studies have been previously performed for LEP and TEVATRON [7, 8] and even for the LHC [9]. Other torsion aspects have

been also recently studied [10, 11]. The LHC, which will have a center-of-mass energy of 14 TeV, will provide unprecedented conditions to investigate many alternative models and will extend the search for new heavy particles up to the 5-6 TeV range, depending on the integrated luminosity obtained. The machine must start its activity at low luminosity ($\mathcal{L} = 10^{-33} \text{cm}^{-2} \text{s}^{-1}$), reaching high luminosity ($\mathcal{L} = 10^{-34} \text{cm}^{-2} \text{s}^{-1}$) after one year of operation [12].

Here we present the discovery potential of torsion field at the LHC. The dielectron channel is used to calculate the luminosity needed for a 5σ discovery as a function of the torsion mass and the fermion-torsion vertex coupling. We consider all the couplings η_f equal. The analysis with early LHC data of new heavy states formed by opposite sign dileptons will have great importance, since these signatures are included in many Standard Model extensions. The LHC experimental data can eliminate or corroborate some of these proposed phenomenological extensions.

In a second part of this work, we present the luminosity needed for the discrimination of the torsion field nature, vectorial or pseudo-vectorial, with 95% C.L.. Finally, we present a variable capable of separating the torsion field from a new vector neutral gauge boson (Z'), predicted by several models, such as the E_6 [13]. We show that, once a signal of a dilepton resonance is experimentally

*Electronic address: asevedo@cern.ch, marroqui@if.ufrj.br

†Electronic address: aline@ufsj.edu.br

found, the accumulated asymmetry (defined in Sec. V) can discriminate between the torsion and the Z' . The parameters and particle efficiencies of the ATLAS detector have been roughly used in this paper, although no detector simulation had been performed.

II. THE TORSION FIELD

There are many experimental and theoretical arguments saying that the minimal Standard Model (SM) is not a complete theory and it should be extended. One possibility is to extend it in such way to include also gravity. This inclusion should predict the observable value of the cosmological constant and bring new observable effects in high energy elementary particle physics. The SM is described using three types of fields: scalar, vectorial and spinorial, by the other hand general relativity has in addition the metric field which describes the geometric property of space-time. A strong candidate to be included in the SM is the space-time torsion field which adds some independent characteristics to the space-time geometry as is shown in the general relativity with torsion [2]. The torsion field can be considered as being composed of three irreducible components: the axial vector S^μ , the vector trace T_α , and the tensor $q_{\beta\mu}^\alpha$.

The general minimal and non minimal action of a Dirac fermion coupled to torsion can be written for practical purposes as [9]

$$S_f = \int d^4x \sqrt{g} \{ i\bar{\psi}\gamma^\mu (\nabla_\mu - i\eta_1\gamma^5 S_\mu + i\eta_2 T_\mu)\psi - m\bar{\psi}\psi \} \quad (1)$$

where η_1 and η_2 are two dimensionless parameters and ∇_μ is the Riemannian covariant derivative (without torsion). The $q_{\beta\mu}^\alpha$ tensor decouples completely from the fermion fields for the minimal and non minimal actions.

One has two approaches: the minimal and the non minimal interaction. The minimal interaction gives $\eta_1 = -1/8$ and the vectorial torsion part decouples completely from the spinor fields. This case is equivalent to put $\eta_2 = 0$ in Eq. 1 and then one has a pure axial vector coupling. So for the minimal case the theory gives a fixed value of η_1 which corresponds to a pure axial vector coupling [2].

By the other hand, the non minimal interaction allows both η_1 and η_2 to have non zero values. In order to simplify our study and analyze the extreme cases, we are

considering the pure axial vector ($\eta_f = \eta_1 \neq 0$ and $\eta_2 = 0$) and the pure vectorial ($\eta_1 = 0$ and $\eta_f = \eta_2 \neq 0$) cases, although the mixed case ($\eta_1 \neq 0$ and $\eta_2 \neq 0$) is not at all excluded. We analyze the non minimal case since the minimal one is very restrictive due to the fixed values of η_1 and η_2 in Eq. 1.

For the axial case, the non minimal interaction of torsion with Standard Model fermions will be given by the following action, where $\psi_{(i)}$ stands for each of the fermions:

$$\mathcal{S}_{A-non-min}^{TS-matter} = i \int d^4x \sqrt{g} \bar{\psi}_{(i)} \left(\gamma^\alpha \nabla_\alpha + i\eta_{1i} \gamma^5 \gamma^\mu S_\mu - im_i \right) \psi_{(i)} \quad (2)$$

While for the vectorial case, the non minimal action will be:

$$\mathcal{S}_{V-non-min}^{TS-matter} = i \int d^4x \sqrt{g} \bar{\psi}_{(i)} \left(\gamma^\alpha \nabla_\alpha - i\eta_{2i} \gamma^\mu T_\mu - im_i \right) \psi_{(i)} \quad (3)$$

where η_{1i} and η_{2i} are the interaction parameters for the corresponding fermion spinor and the subscripts V and A stand for the vectorial and pseudo-vectorial cases. From the theoretical point of view the nonminimal interaction with the geometric vector component of torsion T_μ can not be ruled out [2] and therefore it is worthwhile to work out it in the same manner as it is done with the axial vector component.

We have considered the non minimal parameters equal for all fermions, contrary of what was done on [9] where the top quark coupling was taken to be different from the others due to its larger mass because of the renormalization group running. So, from now on, $\eta_f = \eta_{1i} = \eta_1$, if $\eta_2 = 0$ and $\eta_f = \eta_{2i} = \eta_2$, if $\eta_1 = 0$ then we are dealing with two parameters only, η_f and M_{TS} for the axial and vectorial cases. We are studying the channel $pp \rightarrow e^+e^-$ and this assumption with respect to the top quark coupling makes practically no difference in the results here obtained. This assumption changes slightly the torsion width.

III. EVENT SELECTION

Torsion (TS) described as pure vectorial and pure pseudo-vectorial field was implemented in CompHep event generator [14]. Using this package, we simulate the

process $pp \rightarrow \gamma/Z/TS \rightarrow e^+e^-$ with a center-of-mass energy of 14 TeV and with full interference between the torsion and the SM gauge bosons. The events were generated for three different values of the torsion mass: 1, 3, and 5 TeV and for three values of η_f : 0.2, 0.5 and 0.8, which obeys the limits obtained by [9] and the constraint $M_{TS}/\eta_f \gg m_f$ (or, equivalently, $M_{TS} \gg \eta_f \times m_f$), obtained in [4] for the pure axial case. For the pure T_μ case, there are no such theoretical limits. A cut on the dielectron invariant mass of 500 GeV was applied on generated events in order to reduce the SM background. The CTEQ6L parton distribution functions were employed. The pseudo-rapidities of the electron and the positron were required to be $|\eta| < 2.5$ and each final particle energy should be greater than 5 GeV, both conditions due to the ATLAS detector characteristics. Since in a more realistic scenario jets can be misidentified as electrons in calorimeters, which affect the electron identification, we assume a dielectron identification efficiency of 62%. The overall efficiency, which take into account the cut on η and the electron identification is around 50% [15]. New neutral gauge models based on E_6 were also implemented in CompHep.

IV. TORSION DISCOVERY POTENTIAL AT LHC

In Fig. 1 we present the torsion width as a function of its mass for several fermion-torsion couplings. Due to its huge width, in special for large η_f values, torsion interaction can not be approximated as a contact interaction. Figure 2 shows the production cross section at NNLO for the process $pp \rightarrow \gamma/Z/TS \rightarrow e^+e^-$ as a function of torsion mass and for three different values of η_f . LO cross section obtained with the CompHep package was multiplied by a constant factor $K = 1.35$ in order to take into account the next-to-next-leading order QCD corrections. As expected, the cross section grows as η_f increases, since the fermion-torsion coupling becomes stronger. We can see that for M_{TS} above 4 TeV, there is no significant difference between the cross sections for the different couplings, showing clearly the effect of the parton distribution functions. The widths and total cross-sections are equal for both the pure axial and the pure vectorial cases.

The dielectron channel was chosen to calculate the torsion discovery potential at LHC since ATLAS has a better electron resolution when compared to muon [16]. A signal of a torsion field interacting with the fermions

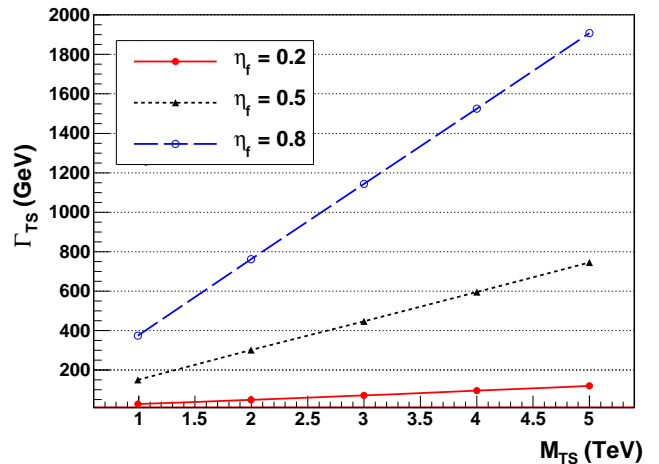


FIG. 1: Torsion widths as a function of torsion mass for several fermion-torsion couplings ($\eta_f = 0.2, 0.5$ and 0.8).

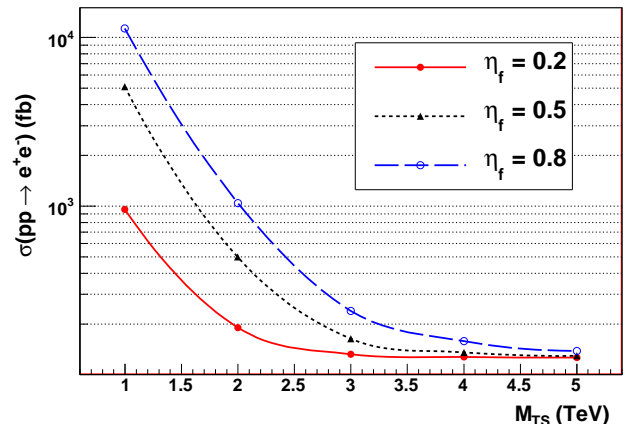


FIG. 2: Torsion production cross section as a function of torsion mass, for several fermion-torsion couplings ($\eta_f = 0.2, 0.5$ and 0.8).

should be observed above the neutral Drell-Yan (DY) process that is the main background in the search of new heavy dilepton resonances. The statistical significance of the torsion signal in the presence of background can be obtained using the likelihood-ratio estimator

$$S_L = \sqrt{2\ln(L_{s+b}/L_b)} \quad (4)$$

where L_{s+b} represents the maximum likelihood value obtained from the unbinned likelihood fit to the dielectron invariant mass assuming that a signal is presented in the data, while L_b is the maximum likelihood value obtained

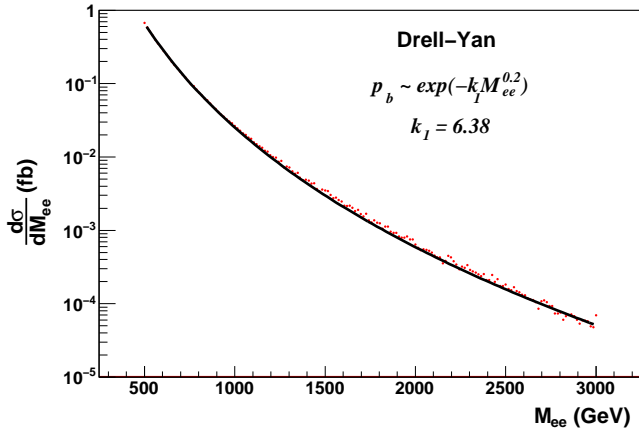


FIG. 3: Background shape determination for $M_{ee} < 3$ TeV

with a background only hypothesis. It has been shown that this estimator has the desired feature of not having an overestimated or underestimated probability of a false discovery [17].

The probability density function (pdf) used to fit the observed dielectron invariant mass spectra is given by [18].

$$p(M_{ee}) = f_s p_s(M_{ee}) + (1 - f_s) p_b(M_{ee}) \quad (5)$$

where p_s is the pdf of the signal, given by a Breit-Wigner distribution, and p_b is the pdf of the background, modeled as exponential functions. The parameters to be fitted are the signal fractions $f_s = N_s/(N_s + N_b)$ (where $N_{s(b)}$ are the number of signal (background) events), the torsion mass M_{TS} peak position and the torsion width Γ_{TS} .

The pdfs that describe the background shape depends on the invariant mass region, and are given by

$$p_b(M_{ee}) \propto \begin{cases} \exp(-k_1 M_{ee}^{0.2}), & \text{if } 500 < M_{ee} < 3 \text{ TeV} \\ \exp(-k_2 M_{ee}), & \text{if } M_{ee} > 3 \text{ TeV} \end{cases} \quad (6)$$

The values of the parameters k_1 and k_2 are obtained from fits to the DY invariant mass Monte Carlo (MC) distribution in the full mass region of interest. Figures 3 and 4 show the fits and the resultant values of k_1 and k_2 : $k_1 = 6.38$ and $k_2 = 0.00209$. We can see that the DY background can be well described by the proposed parametrization.

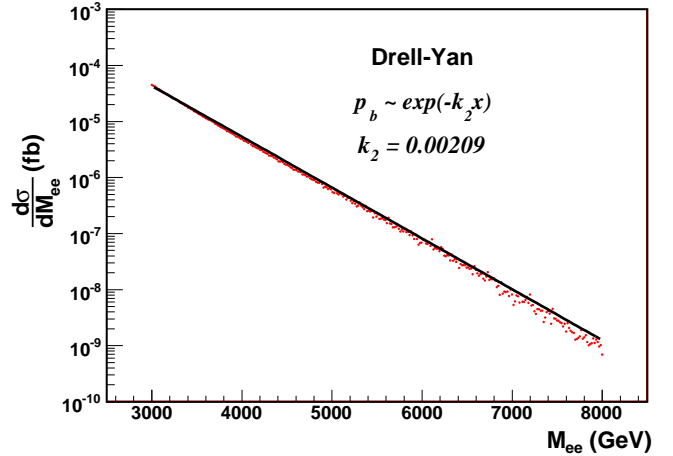


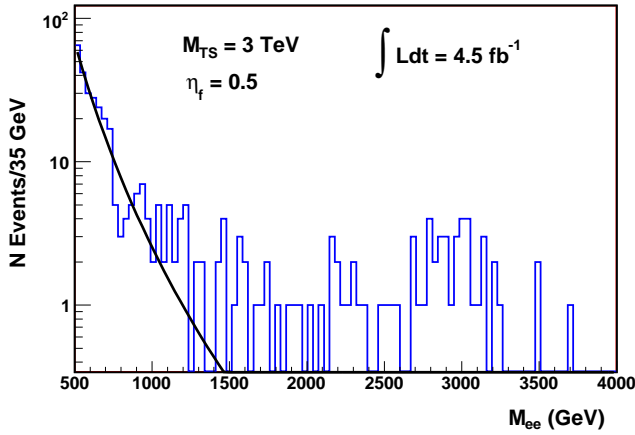
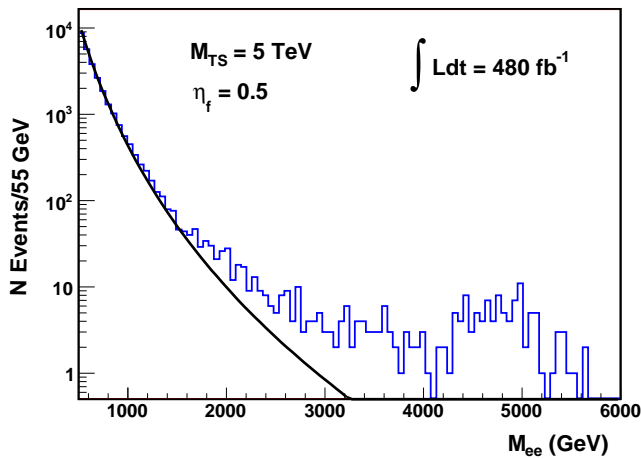
FIG. 4: Background shape determination for $M_{ee} > 3$ TeV

TABLE I: Cuts on M_{ee} obtained from the exponential fit to the invariant mass for different values of M_{TS} and η_f .

	Torsion Mass (M_{TS})		
η_f	1 TeV	2 TeV	5 TeV
0.2	660	1570	3500
0.5	680	1360	3300
0.8	680	1400	3300

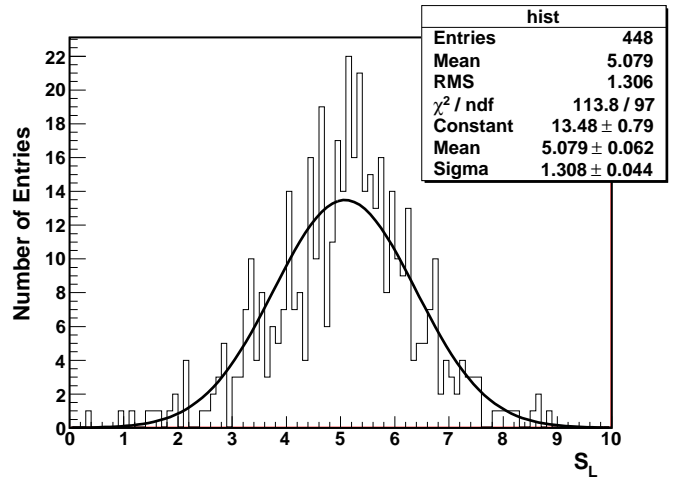
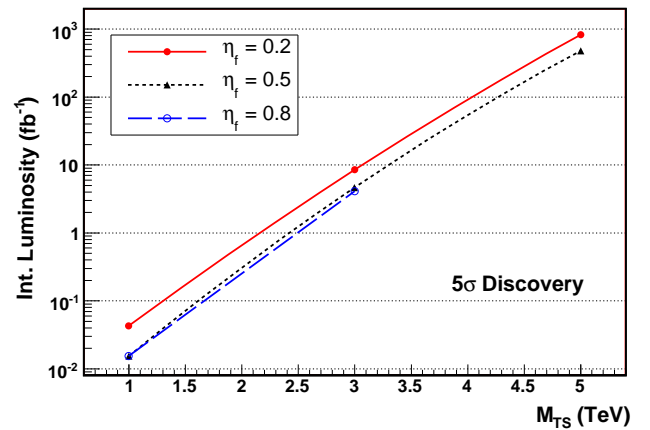
In order to increase the signal-to-background ratio, it was applied a M_{ee} cut to eliminate as much as possible the background contamination on the mass signal. Figures 5 and 6 illustrate for two different values of torsion masses how the cut is obtained: the Equation 6 is used to fit the invariant mass distribution, with $k_{1,2}$ fixed at the values mentioned above, and with the amplitude been the only fitted parameter. The M_{ee} cut is defined as the point where the $d\sigma/dM_{ee}$ reaches the value $0.5 fb$. Table I shows the cut values obtained for the different torsion masses and couplings considered in this study.

To obtain the statistical significance (Eq.4), Equation 5 is fitted to the invariant mass of the events that pass the cut described above. The fit is performed in two steps: first, using Equation 5, we fit the invariant mass for many different MC samples, and take the mean values of M_{TS} and Γ_{TS} from the fitted parameters distribution. Then, fixing M_{TS} and Γ_{TS} at their mean values, we fit the same samples again, under the signal plus background hypothesis (note that in this case, just f_s is fitted), in order to obtain L_{s+b} . By making $f_s = 0$ in Equation 5, which represents the background only hypothesis, we

FIG. 5: Mass cut determination for $M_{TS} = 3$ TeVFIG. 6: Mass cut determination for $M_{TS} = 5$ TeV

fit the same distributions to get L_b . In the last fit the parameters k_1 and k_2 are free. As the result of many fits a S_L distribution is obtained, as illustrated for the case $M_{TS} = 1$ TeV and $\eta_f = 0.2$ in Figure 7. The mean value of S_L distribution is taken as the signal significance for a given luminosity. The value of S_L must be greater than 5 for claiming a discovery.

Fig. 8 shows the integrated luminosity needed for a 5σ discovery as a function of torsion mass for three different values of torsion-fermion couplings. From this plot, we obtain the following conclusions: i) a very low integrated luminosity, of order of 100 pb^{-1} , is needed for discovering a torsion of 1 TeV mass. It means that such signal could be observed at very early days of LHC operation, even in a regime of low luminosity; ii) for a torsion mass of 3

FIG. 7: Significance distribution S_L for $M_{TS} = 1$ TeV and $\eta_f = 0.2$ FIG. 8: Minimum integrated luminosity needed for a 5σ discovery

TeV, the discovery would be possible with an integrated luminosity around 10 fb^{-1} , or approximately 1 year of LHC operation in low luminosity; iii) finally, around 10 years of operation in high luminosity would be needed for the observation of a 5 TeV mass resonance. However, for the case $M_{TS} = 5$ TeV and $\eta_f = 0.8$, no peak can be observed at LHC due to the huge torsion width ($\Gamma_{TS} = 1.9 \text{ TeV}$), although some excess above the DY background can still be identified. For this reason, this particular point is not included in Fig. 8.

V. TORSION NATURE DETERMINATION

We obtain now the minimum integrated luminosity needed to discriminate between the axial and the vectorial models with 95% C. L. as a function of the torsion mass for different η_f values. Assuming that a torsion signal was found at LHC and its mass and width were already experimentally determined, we have considered a mass window for the dielectron invariant mass between $M_{TS}/2$ and $M_{TS} - \Gamma_{TS}$, where M_{TS} and Γ_{TS} are the fitted values for the torsion mass and the torsion width, respectively. This is the region where the interference terms dominate the process.

The pseudorapidity difference $\Delta\eta$ between the electron and the positron can be used to distinguish between the axial and the vectorial torsion models. Due to the energy cuts on the final electron energies ($E_e > 5\text{GeV}$) $\Delta\eta$ is Lorentz invariant. Fig.9 shows the $\Delta\eta$ distribution for $M_{TS} = 3\text{ TeV}$ and $\eta_f = 0.2$ for an integrated luminosity of 165 fb^{-1} . In order to quantify and test the statistical compatibility of the two histograms and since either can have bins with few or even zero contents, we use the $\chi^2 - function$ [19] of $\Delta\eta$ distributions to calculate the minimum integrated luminosity that yields a 95% C.L. discrimination between the axial and vectorial models. Fig.10 shows our results as a function of the torsion mass for $\eta_f = 0.2, 0.5$ and 0.8 . We can see that for $M_{TS} = 1\text{ TeV}$ and $\eta_f = 0.8$, an integrated luminosity of 0.2 fb^{-1} , corresponding to less than one day of LHC data-taking at high luminosity, will be enough to discriminate between axial and vector torsions, while for $M_{TS} = 5\text{ TeV}$ and $\eta_f = 0.2$, an integrated luminosity of 1500 fb^{-1} , corresponding to more than 16 years of LHC data-taking at high luminosity, will be needed to achieve the torsion nature distinction.

VI. TORSION AND NEW NEUTRAL GAUGE BOSON DISCRIMINATION

As the torsion field is characterized by a neutral gauge boson, its mass signal at LHC could be the same of a new heavy neutral resonances, like Z' . In order to identify the signal nature, if its is found, we define an accumulated asymmetry, that is given by the forward-backward asymmetry as a function of M_{ee} evaluated at increasing ranges of the final electron invariant mass M_{ee} . The lower range limit is at a fixed value $M_{TS}/2$ and gradually increasing the upper limit up to $M_{TS} + 500\text{ GeV}$.

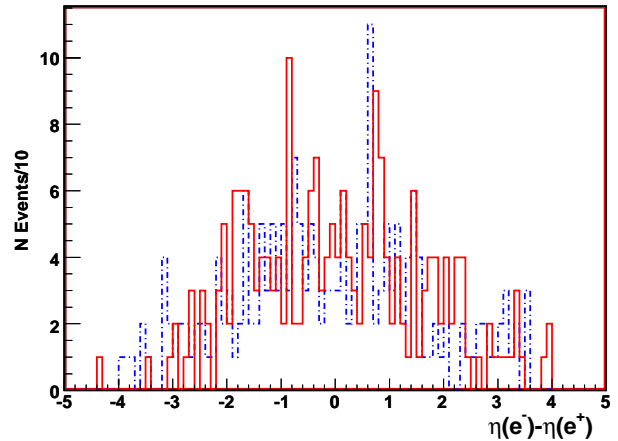


FIG. 9: Pseudorapidity difference between the electron and the positron for axial (solid line) and vectorial (dotted) models, for $M_{TS} = 3\text{ TeV}$ and $\eta_f = 0.2$ for an integrated luminosity of 165 fb^{-1} .

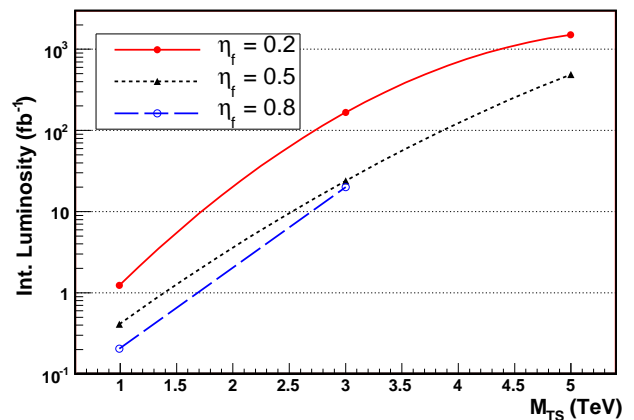


FIG. 10: Minimum integrated luminosity needed for 95% C.L. discrimination between the axial and the vectorial models using the electron-positron pseudorapidity difference distribution.

$$\mathcal{A}(M_{ee}) = \frac{N_F - N_B}{N_F + N_B} \Bigg|_{\frac{M_{TS}}{2}}^{M_{ee}} \quad (7)$$

where N_F is the number of forward events, counted as the number of events with $\cos\theta^* > 0$, and N_B is the number of backward events, which have $\cos\theta^* < 0$, where θ^* is the angle between the outgoing electron and the boost direction at the center of mass frame of the final electrons. The errors of the accumulated asymmetry become

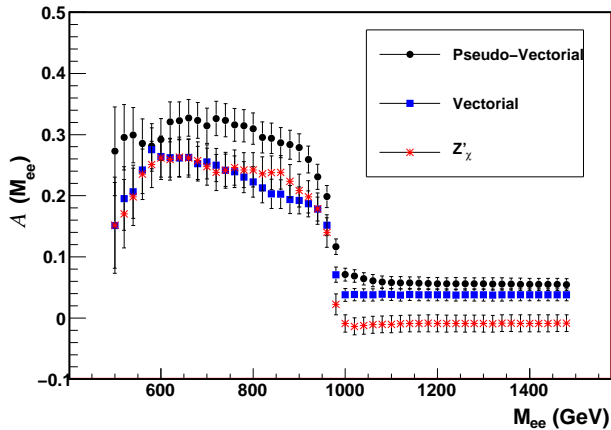


FIG. 11: Discrimination between the axial torsion, vectorial torsion and Z' using the accumulated asymmetry defined in Equation 7 for $M_{TS} = M_{Z'} = 1$ TeV and $\eta_f = 0.2$.

smaller as the invariant mass range increases since the total numbers of events also increases. In order to compare the Z' and torsion fields, we have considered the Z'_χ model, but the analysis can be equally applied to any neutral gauge boson coming from different models.

Figure 11 shows the accumulated asymmetry for the torsion fields (vectorial and pseudo-vectorial) and for Z'_χ , calculated for the case $M_{TS} = M_{Z'} = 1$ TeV, and $n_f = 0.2$ with an integrated luminosity of 20 fb^{-1} . We can see that the Z' can be easily discriminated from the pseudo-vectorial torsion in all range of mass considered.

On the other hand, the Z' curve overlaps the vectorial torsion up to an invariant mass of 1 TeV, but can also be distinguished after that point. Note that it is also possible to distinguish between the vector and pseudo vector torsion fields using this variable. The discriminations are easier for greater values of η_f , since the torsion production cross section increases and therefore the errors are smaller.

In Figures 12 and 13 we see the same distribution for gauge bosons mass of 3 TeV and for $\eta_f = 0.2$ and 0.5 , respectively. In this case, a luminosity of 900 fb^{-1} is needed for discrimination between the resonances. For $\eta_f = 0.2$, the accumulated asymmetry can distinguish Z' and pseudo-vectorial torsion, but has no power to separate the Z' and vectorial torsion. However, this variable shows a good performance on discrimination if $\eta_f = 0.5$, as exhibited in Figure 13.

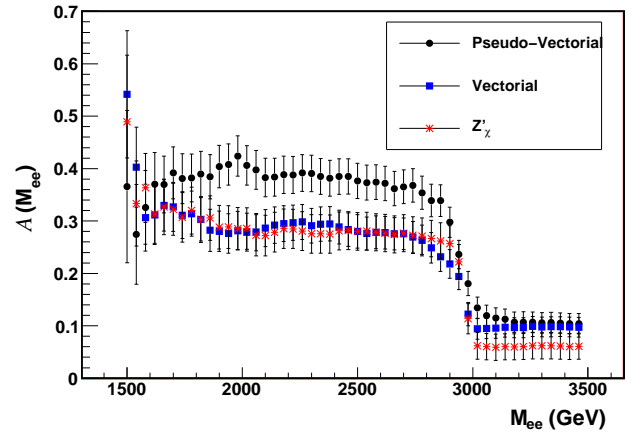


FIG. 12: Same as Fig. 11 but for $M_{TS} = M_{Z'} = 3$ TeV.

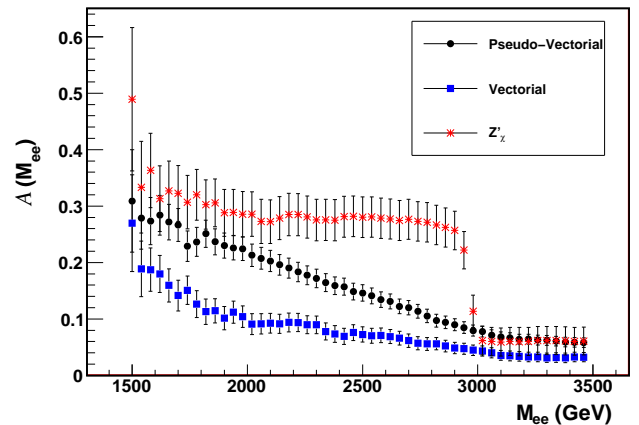


FIG. 13: Same as Fig. 11 but for $M_{TS} = M_{Z'} = 3$ TeV and $\eta_f = 0.5$

VII. CONCLUSIONS

We have studied the phenomenological consequences of a pure axial vector or pure vector torsion action at CERN LHC. In this context, torsion is treated as a massive spin 1 particle, that will form a resonance and will decay into the SM fermions and the model parameters will be the torsion mass (M_{TS}) and the non minimal torsion-fermion couplings (η_f). Using the dielectron channel we have calculated the torsion 5σ discovery at LHC and showed that if such a resonance exists, LHC will be able to detect it after data-taking corresponding to 100 pb^{-1} , if the torsion mass is around 1 TeV or 10 fb^{-1} if the torsion mass is around 3 TeV. Unfortunately, for a torsion mass of 5 TeV and $\eta_f = 0.8$, no peak should be observed due to

torsion huge width.

The initial main focus of LHC will be on discovery, but after this initial phase, focus will turn to model discrimination. Concerning the torsion model, the discrimination will have two main points: the determination of torsion nature (axial vector or vectorial) and the distinction of the torsion field from other new particles predicted by many SM extensions, such the Z' , that will also appear in proton-proton collisions as resonances decaying into difermions. We showed that the pseudorapidity difference of the final electron and positron can be used to distinguish between an axial and a vectorial torsion. As an example, the $\Delta\eta$ will be able to discriminate with 95% C.L. between axial and vector torsions for $M_{TS} = 1$ TeV and $\eta_f = 0.8$, with an integrated luminosity of 0.2 fb^{-1} .

Another variable capable of doing this distinction is the accumulated asymmetry, given by the forward-backward asymmetry value evaluated at different mass ranges. But this asymmetry will require a greater integrated luminosity to achieve the distinction between different torsion natures and is better suited in the discrimination of the torsion fields from an additional neutral gauge boson predicted by the Z'_χ model. When the experimental data be available, combining the two methods will certainly increase the discrimination power of such proposed models.

Acknowledgments: The authors are very grateful to I. L. Shapiro for discussions and suggestions. This work was supported in part by the following Brazilian agencies: CNPq and FAPERJ. AAN thanks to the support given by the HELEN program.

-
- [1] F.W. Hehl *et al.* Rev. Mod. Phys. **48**, 393 (1976).
 - [2] I.L. Shapiro, Phys. Rep. **357**, 113 (2002).
 - [3] R.T. Hammond, Rep. Prog. Phys. **65** 599 (2002).
 - [4] G. de Berredo-Peixoto, J.A. Helayel-Neto and I.L. Shapiro, JHEP **02** (2000) 003.
 - [5] D. Puetzfeld, New Astron.Rev. 49 (2005) 59-64.
 - [6] M. Gasperini, Phys. REv. Lett. 56 (1986) 2873-2876.
 - [7] A.S. Belyaev and I.L. Shapiro, Phys. Lett. B **425**, 246 (1998); Nucl. Phys. **B543**, 20 (1999).
 - [8] U. Mahanta and S. Raychaudhuri, hep-ph/0307350.
 - [9] A.S. Belyaev, I.L. Shapiro and M.A.B. do Vale, Phys. Rev. **D 75**, 034014 (2007).
 - [10] V.A. Kostelecky, N. Russell and J.D. Tasson, Phys. Rev. Lett. **100**, 111102 (2008).
 - [11] S.I. Kruglov, [arXiv:hep-ph/0804.4011].
 - [12] W.H. Smith, [arXiv:hep-ex/0808.3131v1].
 - [13] J.L. Hewett and T.G. Rizzo, Phys. Rep. **183**, 193 (1989).
 - [14] E. Boos *et al.* [CompHEP Collaboration], Nucl. Instrum. Meth. A **534**, 250 (2004). [arXiv:hep-ph/0403113].
 - [15] The ATLAS Collaboration, G. Aad *et al.*, The ATLAS Experiment at the CERN Large Hadron Collider, 2008 JINST 3 S08003.
 - [16] ATLAS Collaboration, Expected Performance of the ATLAS Experiment, Detector, Trigger and Physics, CERN-OPEN-2008-020, Geneva, 2008, to appear.
 - [17] R. Cousins, J. Mumford, V.Y. Value, "Detection of Z' Gauge Bosons in the Dimuon Decay Mode in CMS", CMS-NOTE-2005-002, Geneva, 2005.
 - [18] R. Cousins, J. Mumford, V.Y. Value, "Detection of Z' Gauge Bosons in the Dimuon Decay Mode in CMS", CMS-NOTE-2006-062, Geneva, 2006.
 - [19] F.M.L. Almeida Jr., M. Barbi and M.A.B. do Vale, Nucl. Instrum. and Meth.A **449**,383-395 (2000).